coatings

MDPI

Article

A Surface Photovoltage Study of Surface Defects on Co-Doped TiO_2 Thin Films Deposited by Spray Pyrolysis

Henry Wafula [1,*], Albert Juma [2], Thomas Sakwa [1], Robinson Musembi [3] and Justus Simiyu [3]

1 Department of Physics, Masinde Muliro University of Science and Technology, P.O. Box 190, Kakamega 50100, Kenya; tsakwa@mmust.ac.ke
2 Department of Physics and Astronomy, Botswana International University of Science and Technology, Private Bag 16, Palapye, Botswana; jumaa@biust.ac.bw
3 Department of Physics, University of Nairobi, P.O. Box 30197, Nairobi 00100, Kenya; musembirj@uonbi.ac.ke (R.M.); simiyuj@uonbi.ac.ke (J.S.)
* Correspondence: hbarasa@mmust.ac.ke; Tel.: +254-775-973-286

Academic Editor: Alessandro Lavacchi
Received: 20 May 2016; Accepted: 14 July 2016; Published: 22 July 2016

Abstract: Surface photovoltage (SPV) spectroscopy is a powerful tool for studying electronic defects on semiconductor surfaces, at interfaces, and in bulk for a wide range of materials. Undoped and Cobalt-doped TiO_2 (CTO) thin films were deposited on Crystalline Silicon (c-Si) and Flourine doped Tin oxide (SnO_2:F) substrates by chemical spray pyrolysis at a substrate temperature of 400 °C. The concentration of the Co dopant in the films was determined by Rutherford backscattering spectrometry and ranged between 0 and 4.51 at %. The amplitude of the SPV signals increased proportionately with the amount of Co in the films, which was a result of the enhancement of the slow processes of charge separation and recombination. Photogenerated holes were trapped at the surface, slowing down the time response and relaxation of the samples. The surface states were effectively passivated by a thin In_2S_3 over-layer sprayed on top of the TiO_2 and CTO films.

Keywords: doping; photovoltage; spray pyrolysis

1. Introduction

Surface photovoltage (SPV) spectroscopy is a non-destructive and fast technique for investigating optoelectronic properties at surfaces, interfaces, and in bulk by monitoring the illumination-induced changes in the surface voltage [1]. It provides important information, such as surface band bending, surface and bulk carrier separation and recombination, surface state distribution, and defect states by studying the photo-induced carrier separation and transfer in semiconductor materials. SPV has been used to study nanocrystalline semiconductors for various applications, and has recently received renewed attention for the study of integrated devices and micro-heterogeneous systems [2–4].

Doping of metal oxides with transition metals has led to the investigation of new materials with ferromagnetic properties for application in Spintronics devices, photocatalytic applications, as well as for energy conversion and storage [5–8]. Co dopant is optically active, imparts magnetic properties to TiO_2 suitable for Spintronics device application, and enhances photocatalytic activity through the introduction of additional electronic defects in its lattice [9–12]. A few Co atoms are sufficient to create specific defect structures that trap charge carriers and induce ferromagnetic properties in TiO_2 [11]. The enhancement of photocatalytic activity of Co-doped TiO_2 (CTO) is associated with the red shift of the band gap due to the sp-d exchange interaction between band electrons and localized d electrons of the Co^{2+} substituting for Ti^{4+} cations, which shifts the conduction band downwards and the valence band upwards [13,14]. The red shift has also been associated with an increase in the density of defects,

resulting in the formation of impurity bands, which may spread and overlap with the conduction band [5].

Anatase TiO_2 consists of interconnected TiO_6 octahedron, each in contact with eight neighbors via four corners and four edges. Local distortion in the octahedron induces energy levels below the conduction band. Incorporation of Co—which has a larger ionic radius than Ti—introduces additional distortions, increasing the density of defects [15]. Co^{2+} dopant substitutes for Ti^{4+}, creating additional oxygen vacancies, which leave behind a lone electron pair. The electron pair reduces two Ti^{4+} ions to Ti^{3+}. The oxygen defects are formed on the surface and in the bulk on TiO_2. The vacancies in the bulk are less stable and may migrate to the surface. The oxygen vacancies, which act as electron donors, can be associated with both deep and shallow defects. The enhanced paramagnetic properties in Co-doped TiO_2 have been linked to increased density of oxygen vacancies [9–15]. Co^{2+} defects are also introduced in the mid-gap near the oxygen and Ti^{3+}-related trap states. Trap-to-trap transition of electrons can take place from a defect to a Co^{2+} state, from where they relax to ground state [10].

The electronic, structural, and electrical properties of thin films depend on the deposition methods. CTO films and nanostructures have been deposited by sol–gel [9,10], ball milling [14], spray pyrolysis [16,17], solvo-thermal [15], pulsed laser deposition [18,19], molecular beam epitaxy [20], reactive co-sputtering [21], and atomic layer deposition [22]. Chemical spray pyrolysis has the advantage that it is vacuum-free, allows for a wide variety of precursor choices and deposition parameters, and different precursor solutions can be mixed in different proportions before deposition to effectively dope the samples.

In this work, CTO thin films were prepared by spray pyrolysis from precursors with different compositions of Ti and Co salts. The composition was analyzed by Rutherford backscattering spectrometry (RBS), while optoelectronic properties were investigated using UV-Vis and SPV techniques. SPV is a photoelectric method that is very sensitive to changes in electronic states participating in charge separation, independent of whether it is at the surface, interface, or in the bulk [23].

2. Materials and Methods

To prepare the precursor solutions, 19.2 mL of Titanium isopropoxide (TTIP) was mixed with 28.8 mL of 2,4-Pentanedione solution. Absolute ethanol solvent was added and stirred to make 480 mL of solution. This was called solution A. Solution B was prepared by dissolving 43.2 mg of anhydrous $CoCl_2$ in 50 mL of acetonitrile and stirring for 3 hrs. Different volumes of solution B were added to solution A in volumetric percentages varying from 0% to 50%. TiO_2 films were obtained from solution A and Co-doped TiO_2 (CTO) thin films from the mixture of solutions A and B by spraying for 5 min at a substrate temperature of 400 °C. RBS experiments were performed using a 2.0 MeV He^+ ion beam at zero incidence and exit angle of 12°. The backscattered ions were detected at a scattering angle of 168°. The charge was 5 coulombs with measurement time of about 12 min. The optoelectronic defects were investigated by modulated surface photovoltage in the fixed parallel capacitor configuration [24,25], with the incident light modulated at 8 Hz. The SPV signals were detected using a high impedance buffer and a lock-in amplifier.

3. Results

3.1. Compositional Analysis

Figure 1a shows the RBS spectra for the TiO_2 and CTO thin films deposited on Crystalline Silicon (c-Si) substrates. The RBS signals from Co, Ti, Si substrate, and O were identified as indicated in the figure. The channel position of these signals depends on the atomic number of the elements detected. The heavier elements appear at higher channel numbers, corresponding to higher energy of the backscattered He^+ ions after collision with the nucleus of that specific atom. The height/yield of the RBS signal is proportional to the amount of material present in the sample, and it depends on the

scattering cross-section of the detected element. The width of the peak is proportional to the thickness of the probed sample and depends on the energy loss per unit depth of the detected element [26].

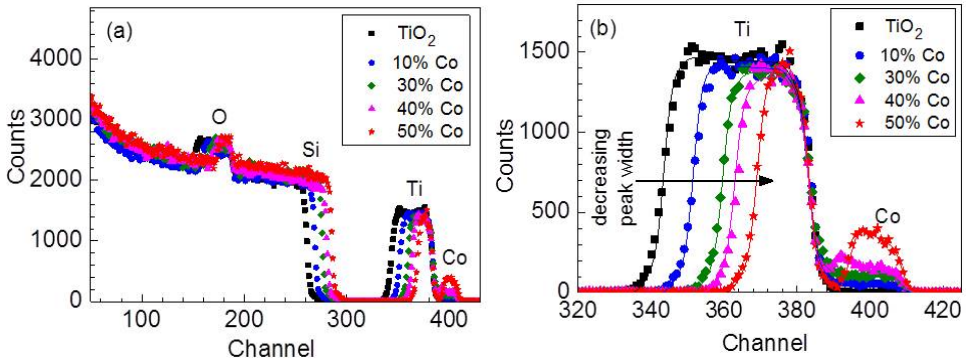

Figure 1. (**a**) Rutherford backscattering spectrometry (RBS) spectra; and (**b**) Ti and Co RBS signals for the TiO_2 and Cobalt-doped TiO_2 (CTO) thin films doped with Co concentrations of 0, 10, 20, 30, 40, and 50% by volume of $CoCl_2$ dopant solution.

A decrease in the width of the RBS signals from Ti and Co and a shift of the signal from the surface of the c-Si substrate to higher channels was observed with an increase in the amount of $CoCl_2$ in the precursor solution. A decrease in the width of the RBS signal is concomitant with a decrease in the film thickness. The height of the Co signal increased as a function of increasing amount of solution B in the precursor, which confirms the increase in the amount of Co in the CTO film. Figure 1b shows the Ti and Co signals from the RBS spectra fitted using Spewa software (Version 1.0, Institute of solid state Physics, Jena, Germany) based on the Nuno's Data Furnace (NDF) code [27].

The thicknesses and atomic concentrations of the TiO_2 and CTO thin films were extracted from fitting the spectra and from the integrals of the Ti and Co signals. The thickness for undoped TiO_2 was 175 nm, and for the CTO films it ranged between 175 nm for 5 vol % and 60 nm for 50 vol % of $CoCl_2$ in the precursor solution, as given in Table 1. The film deposition rate was dependent on the composition of the precursor solution, and decreased with an increase in the amount of $CoCl_2$ in the solution. The Co atomic concentrations in the thin films obtained from fitting the RBS spectra as shown in Figure 1b amounted to between 0.43 at % and 4.51 at % for CTO films deposited from solutions containing 5 vol % and 50 vol % of $CoCl_3$, respectively, as presented in Table 1.

Table 1. Thin film thickness and Co dopant concentrations as a function of the $CoCl_2$ vol % in the precursor solution.

$CoCl_2$ vol %	Thickness (nm)	Co (at %)
0	175	0
5	175	0.43
10	140	0.60
20	140	1.25
30	105	1.50
40	90	2.40
50	60	4.51

3.2. Modulated Charge Separation

The electronic defects in TiO_2 and CTO thin films deposited on SnO_2:F substrates were investigated by studying photogenerated charge separation under chopped light. In modulated SPV experiments, four signals are normally recorded using a lock-in amplifier. The in-phase (X-signal) and the phase shifted by 90° (Y-signal) with respect to the reference modulated signal gives information

about the direction of separation of the photogenerated charge carriers and the time response of the sample to the modulation of the incident light. The spectral dependent SPV amplitude is the square root of the sum of the squares of the X and Y signals, while the phase angle is the inverse tangent of the ratio between the Y and X signals [27,28].

Figure 2a shows SPV amplitudes for the TiO_2 and CTO thin films doped with 0.43, 0.60, 1.25, and 2.40 at % of Co. The onset energy of the signal was 0.96 eV for all samples (which is very low), compared to the absorption edge of TiO_2 which has a band gap of 3.2 eV. The onset energy of the SPV signal is characteristic of the mobility edge and is expected to be close to the band gap energy for an ideal semiconductor. The SPV signal was therefore dominated by charge separation below the TiO_2 band gap, which indicates the possibility of there being a high density of sub-band gap defect states.

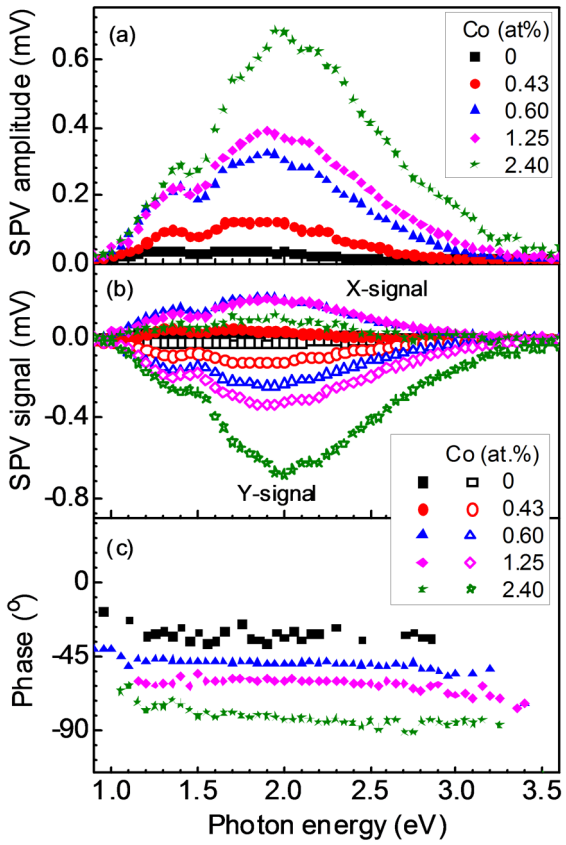

Figure 2. (**a**) Modulated surface photovoltage (SPV) amplitude; (**b**) X- and Y- signals; and (**c**) phase angles for TiO_2 and CTO thin films with Co dopant concentrations of 0.43, 0.60, 1.25, and 2.40 at %.

The amplitude signal shows two peaks centered at 1.4 and 1.9 eV. Such peaks cannot be related to absorption peaks or peaks observed in spectroscopy, because the generation of an SPV signal could be a net result of several charge separation and recombination processes [28]. The two peaks therefore relate to energetic sub-band gap defects participating in charge separation and relaxation processes. The magnitude of the SPV amplitude at 1.9 eV increased from 0.036 mV for undoped TiO_2 to 0.13, 0.32, 0.40, and 0.70 mV for dopant concentrations of 0.43, 0.60, 1.25, and 2.40 at %, respectively, while the film thickness decreased. The SPV amplitude is proportional to the number of photogenerated charge carriers separated in space, and the perpendicular distance between them. The magnitude of the SPV signal was not proportional to the film thickness, so it follows that the increase in the SPV amplitude was not due to an increase in the charge separation distance, but probably due to an increase in the density of the photogenerated charge carriers.

If the charge separation is caused by only one mechanism and the relaxation is due to recombination, the X and Y signals will have opposite signs [24,25,28], as shown in Figure 2b. The X-signal is positive, while the Y-signal is negative, indicating preferential separation of photogenerated electrons towards the substrate and holes towards the top surface. The X signal increased from 0.03 mV to 0.20 mV when the Co concentration in the film was increased from zero to 1.50 at %, but then dropped to 0.10 mV for higher Co amounts. There was no direct relationship between the Co concentration and magnitude of the X signal.

The absolute magnitude of the Y signal increased from 0.01 mV for undoped TiO_2 to 0.11, 0.23, 0.32, and 0.67 mV when the amount of Co was increased to 0.6, 1.25, 1.50, and 2.4 at %, as shown in Figure 2b. This shows a direct correlation between the magnitude of the Y signal and the Co concentration in the CTO films. It can be concluded that the systematic increase in the SPV amplitude observed in Figure 2a with the increase in Co was mainly due to the concomitant increase in the Y signal. The Y-signal characterizes the phase shift between the SPV signal and the chopped light, and it corresponds to the slow increase or decrease of the SPV signal in relation to the half period of modulation [28]. The increase in the Y signal implies that the charge separation and/or relaxation were much slower than the modulation period of the chopped light. It follows that an increase in the Co dopant in the films slows down the charge separation and recombination processes.

Incorporation of Co ions introduces distortions in the octahedron of the TiO_2 structure due to the difference in the ionic radii of Ti (0.605 Å) and Co (0.745 Å), enhancing the density of defect states and the concentration of the photogenerated charge carriers in the different trap levels [15]. Photoluminescence studies have shown that Co doping of TiO_2 increases the lifetime of photogenerated carriers by introducing mid-band gap trap states associated with d states of cobalt, where an increase in the relaxation time of conduction electrons is observed before it undergoes recombination [10]. This explains the increase in the Y-signal with increasing Co dopant discussed above.

The phase angle of the SPV signal gives information about the direction of charge separation and the time response of the sample in relation to the period of modulation. For example, a positive X signal and a phase angle between 0° and -90° implies a single charge separation process with photogenerated electrons separated preferentially towards the internal interface [29]. In Figure 2c, the phase angle was observed to shift from -30° for undoped TiO_2 to -48°, -60°, and -80°, with an increase in Co concentration to 0.6 at %, 1.25 at %, and 2.40 at %, respectively. A shift of the phase angle towards -90° means that the charge separation and/or relaxation processes became slower with increasing Co concentration [29–32].

The phase angle was independent of the photon energy, and so it can be concluded that in all samples, there was only one transport mechanism involved with charge separation and recombination processes within this spectral range. The shift in the phase angle corresponds to the increase in the Y-signal to more negative values, as discussed above (Figure 2b). The response times of the CTO samples to modulated light were increased by Co-doping. This could be due to enhanced trapping of the photogenerated holes in surface defect states.

Figure 3 shows the SPV signals of the bare In_2S_3 and CTO/In_2S_3 multilayer as a function of the Co concentration in the thin films. The onset of the SPV signal was 2.0 eV for bare In_2S_3 and 1.92 eV for TiO_2/In_2S_3 and all CTO/In_2S_3 samples, independent of the Co concentration. The optical band gap of Ion Layer Gas Reaction deposited In_2S_3 thin films similar to those prepared in this work has been reported to be 2.0 eV [23]. The formation of SPV signal below the In_2S_3 band gap was therefore due to charge separation involving tail states below the In_2S_3 band gap and probably due to defect states at the CTO/In_2S_3 interface. The magnitude of the SPV amplitude (Figure 3a) of the TiO_2/In_2S_3 was almost twice that of the CTO/In_2S_3 films. The SPV amplitude below 2.3 eV is higher for the TiO_2/In_2S_3 and CTO/In_2S_3 multilayer's compared to that of the bare In_2S_3 films, while there was barely any signal below 1.7 eV for all samples. There was dependence of the SPV signal on the Co dopant concentration. Compared to the SPV signals from the bare TiO_2 and CTO films in Figure 2, we can conclude that the shallow defects centered at 1.4 eV were effectively passivated by the In_2S_3 over-layer.

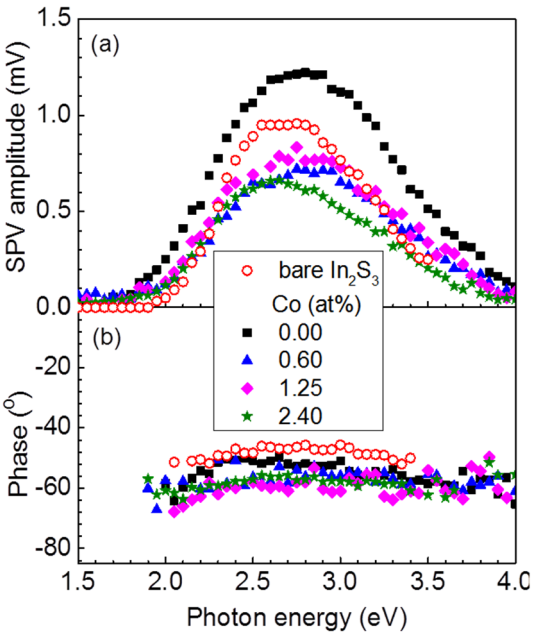

Figure 3. (**a**) Modulated SPV amplitude; and (**b**) phase angles for TiO_2 and CTO thin films doped with 0.6 at %, 1.25 at %, and 2.40 at % of Co.

The X signal was positive and the Y signal negative, which confirmed that the photogenerated electrons were preferentially separated toward the substrate and holes towards the surface. The phase angle for In_2S_3 was -47°, but shifted to about -60° for all the CTO/In_2S_3 samples (Figure 3b). This means that charge separation and recombination processes were slower for CTO/In_2S_3 samples compared to bare In_2S_3 films. The interface states at CTO/In_2S_3 heterojunctions played a role in the generation of the SPV signal in these samples by slowing down the processes.

3.3. Band Gap Diagram for CTO/In_2S_3 Double Layer

Charge separation across the CTO/In_2S_3 interface can be understood using the band diagram given in Figure 4. The band gap of TiO_2 was taken as 3.2 eV and that of In_2S_3 as 2.0 eV. Figure 4a indicates the presence of energetic surface defects centered at 1.9 and 1.4 eV below the conduction band, as deduced from Figure 2a. When the sample is illuminated, photon energies in this range are absorbed and the electrons trapped in this energetic defect state get excited into the conduction band, resulting in the SPV signal peaking at 1.4 and 1.9 eV. Photogenerated electrons excited into the conduction band are drawn into the bulk and holes towards the surface by the electric field created by the charge separation. The holes can be trapped at the surface states, resulting in delayed recombination. This is detected as an increase in the SPV Y-signal or an increase in the relaxation time of the conduction electrons in Photoluminescence measurements [6]. Increasing the Co dopant concentration enhanced the density of the surface states, where a larger number of holes got trapped, resulting in the higher amplitude of the Y-signal with increasing dopant amount, as observed in Figure 2b.

Introduction of Co^{2+} ions into a TiO_2 lattice is known to induce structural distortion and hence an increase of defect states. Because Co^{2+} is incorporated with a charge of +2, oxygen vacancies are created to fulfill the charge neutrality condition [5]. Surface trap states have been attributed to the Ti^{3+} trap states and oxygen vacancies. Photoluminescence experiments have shown radiative recombination of trapped electrons at 0.7–1.6 eV below the conduction band edge of TiO_2, which are associated with uncoordinated Ti^{3+} defects. Distribution of hole traps energetically positioned at 2.5–1.8 eV below the band gap are associated with hole traps due to oxygen vacancies [33–35]. Oxygen vacancies can form both shallow donor states as well as relatively deep trap levels located on the surface of TiO_2. The defect states observed at 1.4 eV can be assigned to acceptor-like electron traps resulting from the Ti^{3+}

defects, while the donor-like states localized at 1.9 eV below the conduction band can be associated with oxygen vacancies. With Co doping, the new oxygen vacancies create lone pair electrons in the vicinity of Ti^{4+} and reduce it to Ti^{3+}, increasing the density of both oxygen vacancy and Ti^{3+} defect states [33].

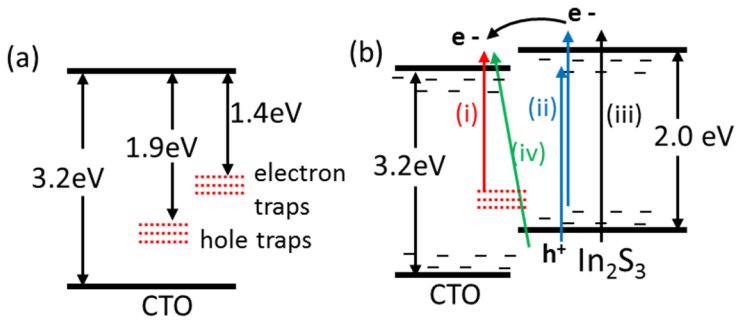

Figure 4. The band diagram of (**a**) bare TiO_2 and CTO layers; and (**b**) CTO/In_2S_3 double layer.

By covering the TiO_2 and CTO films with a thin In_2S_3 over-layer, the electronic defects on the surfaces were passivated and the SPV signals below the band gap disappeared. The SPV signal observed below the In_2S_3 band gap in Figure 3 was due to interface states existing at the CTO/In_2S_3 heterojunctions, which were not fully passivated. Some deep trap states remained at the interface and contributed to charge separation. As shown in Figure 4b, the SPV signal measured from the CTO/In_2S_3 double layer was due to several charge separation processes—namely, (i) photon absorption and excitation of electrons from the CTO/In_2S_3 interface states into the CTO conduction band; (ii) charge separation involving In_2S_3 tail states; (iii) band-to-band absorption in In_2S_3; and (iv) excitation from In_2S_3 valence band into CTO conduction band. It is also possible to have electrons excited from the defects states below the In_2S_3 band gap to states below TiO_2 band gap. The SPV measurement does not distinguish between the different processes because it only captures the net charge separation mechanisms.

It can be concluded that the enhancement of the photocatalytic activity of CTO films and nanostructures observed in visible light is mainly due to an increase in the surface defects that are involved in charge separation. Substitution of Ti^{4+} by Co^{2+} causes distortions in the lattice structure and the creation of additional oxygen vacancies, which increases the density of the deep and shallow defect states in CTO films [15]. Co doping does not introduce new electronic defects, but increases the density and distribution of the already existing Ti^{3+} and oxygen vacancy defects. This behavior has led to an increase in the possible applications of TiO_2 doped with transition metals in optoelectronics, especially under visible light.

4. Conclusions

Increasing the amount of Co dopant in the TiO_2 thin film resulted in a decrease in the deposition rates. The optoelectronic properties of the CTO films showed dependence on the concentration of the Co dopant. The increase in the amplitude of the SPV signal was due to enhanced charge trapping by the surface defect states created by the substitution of Ti^{4+} by Co^{2+} in the TiO_2 lattice. The formation of the SPV signal in the CTO/In_2S_3 double layer resulted mainly from charge separation in the In_2S_3 due to photon absorption and the excitation of electrons from the valence band into the conduction band of the In_2S_3 over-layer. The SPV onset energy of the CTO/In_2S_3 layers (1.92eV) was close to but slightly lower than the band gap of In_2S_3 (2.0 eV), and this can be due to the excitation of electrons from tail states below the band gap of In_2S_3. The holes can be trapped at the surface states, resulting in delayed recombination. This is detected as an increase in the SPV Y-signal or an increase in the relaxation time of the conduction electrons in PL measurements. This explains the enhanced photocatalytic activity in CTO films and nanostructures compared to undoped TiO_2 reported in literature.

Acknowledgments: Authors appreciate the financial support from Deutscher Akademischer Austausch Dienst (DAAD), Christian.-Herbert. Fischer for laboratory space during sample preparation, technical support by Barth and constructive discussions with Elke. Wendler.

Author Contributions: Henry Wafula and Albert Juma conceived, designed, performed the experiments and wrote the paper; Robinson Musembi, Thomas Sakwa and Justus Simiyu analyzed the data.

Conflicts of Interest: The authors declare no conflict of interest. The sponsors had no role in the design of the study; in the collection, analysis, or interpretation of data; in the writing of the manuscript, and in the decision to publish the results.

References

1. Kronik, L.; Shapira, Y. Surface photovoltage phenomena: Theory, experiments and applications. *Surf. Sci. Rep.* **1999**, *37*, 1–206. [CrossRef]
2. Liqianga, J.; Xiaojun, S.; Jing, S.; Weimin, C.; Zili, X.; Yaoguo, D.; Honggang, F. Review of surface photovoltage spectra of nanosized semiconductor and its applications in heterogeneous photocatalysis. *Sol. Energy Mater. Sol. Cells* **2003**, *79*, 133–151. [CrossRef]
3. Zhao, J.; Osterloh, F. Photochemical charge separation in nanocrystal Photocatalyst films: Insights from surface photovoltage spectroscopy. *J. Phys. Chem. Lett.* **2014**, *5*, 782–786. [CrossRef] [PubMed]
4. Rotschild, A.; Levakov, A.; Shapira, Y.; Ashkenasy, N.; Komem, Y. Surface photovoltage spectroscopy study of reduced and oxidized nanocrystalline TiO_2 films. *Surf. Sci.* **2003**, *532–535*, 456–460. [CrossRef]
5. Ali, B.; Shah, L.; Ni, C.; Xiao, J.; Shah, S. Interplay of dopant, defects and electronic structure in driving ferromagnetism in Co-doped oxides: TiO_2, CeO_2 and ZnO. *J. Phys. Condens. Mater.* **2009**, *21*, 456005. [CrossRef] [PubMed]
6. Tatlıdil, I.; Bacaksız, E.; Kurtulus, C.; Buruk, C.; Breen, C.; Sokmen, M. A short literature survey on iron and cobalt ion doped TiO_2 thin films and photocatalytic activity of these films against fungi. *J. Alloys Compds.* **2012**, *517*, 80–86. [CrossRef]
7. Mital, G.; Manoj, T. A review of TiO_2 nanoparticles. *Chin. Sci. Bull.* **2011**, *56*, 1639–1657.
8. García-Mota, M.; Vojvodic, A.; Abild-Pedersen, F.; Nørskov, J. Electronic origin of the surface reactivity of transition-metal-doped TiO_2 (110). *J. Phys. Chem.* **2013**, *117*, 460–465. [CrossRef]
9. Barakat, M.; Hayes, G.; Shah, S. Effect of cobalt doping on the phase transformation of TiO_2 nanoparticles. *J. Nanosci. Nanotechnol.* **2005**, *5*, 759–765. [CrossRef] [PubMed]
10. Choudhury, B.; Choudhury, A. Luminescence characteristics of cobalt doped TiO_2 nanoparticles. *J. Lumin.* **2012**, *132*, 178–184. [CrossRef]
11. Roberts, K.; Varela, M.; Rashkeev, S.; Pantelides, S.; Pennycook, S.; Krishnan, K. Defect-mediated ferromagnetism in insulating Co-doped anatase TiO_2 thin films. *Phys. Rev. B* **2008**, *78*, 014409. [CrossRef]
12. Kim, J.; Park, J.; Park, B.; Noh, H.; Oh, S.; Yang, J.; Kim, D.; Bu, S.; Noh, T.; Lin, H.; et al. Ferromagnetism induced by clustered Co in Co-doped anatase TiO_2 thin films. *Phys. Rev. Lett.* **2003**, *90*, 017401. [CrossRef] [PubMed]
13. Sadanandam, G.; Lalitha, K.; Kumari, V.; Shankar, M.; Subrahmanyam, M. Cobalt doped TiO_2: A stable and efficient photocatalyst for continuous hydrogen production from glycerol: Water mixtures under solar light irradiation. *Int. J. Hydrog. Energy* **2013**, *38*, 9655–9664. [CrossRef]
14. Santara, B.; Pal, B.; Giri, P. Signature of strong ferromagnetism and optical properties of Co-doped TiO_2 nanoparticles. *J. Appl. Phys.* **2011**, *110*, 114322. [CrossRef]
15. Das, K.; Sharma, S.; Kumar, M.; De, S. Morphology dependent luminescence properties of Co doped TiO_2 nanostructures. *J. Phys. Chem.* **2009**, *C113*, 14783–14792. [CrossRef]
16. Karimipour, M.; Mageto, M.; Etefagh, R.; Azhir, E.; Mwamburi, M.; Topalian, Z. Room temperature magnetization in Co-doped anatase phase of TiO_2. *Eur. Phys. J. Appl. Phys.* **2013**, *61*, 10601. [CrossRef]
17. Sharma, S.; Chaudhary, S.; Kashyap, S. Observation of room temperature ferromagnetism in spray pyrolyzed polycrystalline $Ti_{1-x}Co_xO_2$ thin films. *J. Phys. D: Appl. Phys.* **2010**, *43*, 015007. [CrossRef]
18. Escobar-Alarcón, L.; Pérez-Álvarez, J.; Solís-Casados, D.; Camps, E.; Romero, S.; Jiménez-Becerril, J. Preparation of Co:TiO_2 thin films by crossed-beam pulsed laser deposition. *Appl. Phys. A* **2013**, *110*, 909–913. [CrossRef]
19. Nguyen, H.; Prellier, W.; Sakai, J.; Ruyter, A. Substrate effects on room temperature ferromagnetism in Co-doped TiO_2 thin films grown by pulsed laser deposition. *J. Appl. Phys.* **2004**, *95*, 7378–7380. [CrossRef]

20. Murakami, M.; Matsumoto, Y.; Hasegawa, T.; Ahmet, P.; Nakajima, K.; Chikyow, T.; Ofuchi, H.; Nakai, I.; Koinuma, H. Cobalt valence states and origins of ferromagnetism in Co doped TiO_2 rutile thin films. *J. Appl. Phys.* **2004**, *95*, 5330–5333. [CrossRef]
21. Park, W.; Ortega-Hertogs, R.; Moodera, J.; Punnoose, A.; Seehra, M. Semiconducting and ferromagnetic behavior of sputtered Co-doped TiO_2 thin films above room temperature. *J. Appl. Phys.* **2002**, *91*, 8093–8095. [CrossRef]
22. Pore, V.; Dimri, M.; Khanduri, H.; Stern, R.; Lu, J.; Hultman, L.; Kukli, K.; Ritala, M.; Leskelä, M. Atomic layer deposition of ferromagnetic cobalt doped titanium oxide thin films. *Thin Solid Films* **2011**, *519*, 3318–3324. [CrossRef]
23. Juma, A.O.; Azarpira, A.; Steigert, A.; Pomaska, M.; Fischer, C.-H.; Lauermann, I.; Dittrich, T. Role of chlorine in In_2S_3 for band alignment at nanoporous-TiO_2/In_2S_3 interfaces. *J. Appl. Phys.* **2013**, *114*, 053711. [CrossRef]
24. Andreas, K.; Robin, H.; Michael, G. Artificial Photosynthesis Investigation on the Mechanism of Photosensitization of Nanocrystalline TiO_2 Solar cells by Chlorophyll Derivatives. *J. Phys. Chem.* **1994**, *98*, 952–959.
25. Duzhko, V.; Timoshenko, V.; Koch, F.; Dittrich, T. Photovoltage in nanocrystalline porous TiO_2. *Phys. Rev. B* **2001**, *64*, 075204. [CrossRef]
26. Prajongtat, P.; Dittrich, T. Precipitation of $CH_3NH_3PbCl_3$ in $CH_3NH_3PbI_3$ and its impact on modulated charge separation. *J. Phys. Chem. C* **2015**, *119*, 9926–9933. [CrossRef]
27. Chu, W.; Mayer, J.; Nicolet, M. *Rutherford Backscattering Spectrometry*; Academic Press Inc.: San Diego, CA, USA, 1978.
28. Jeynes, C.; Barradas, N.P.; Rafla-Yuan, H.; Hichwa, B.P.; Close, R. Accurate depth profiling of complex optical coatings. *Surf. Interface Anal.* **2000**, *30*, 237–242. [CrossRef]
29. Juma, A.O. Copper diffusion in In_2S_3 and charge separation at In_2S_3/CuSCN and TiO_2/In_2S_3 interfaces. Ph.D. Thesis, Freie Universitaet, Berlin, Germany, 2013.
30. Kaushik, A.; Dalela, B.; Kumar, S.; Alvi, P.A.; Dalela, S. Role of Co doping on structural, optical and magnetic properties of TiO_2. *J. Alloys Compds.* **2013**, *552*, 274–278. [CrossRef]
31. Kykyneshi, R.; McIntyre, D.H.; Tate, J.; Park, C.H.; Keszler, D.A. Electrical and optical properties of epitaxial transparent conductive BaCuTeF thin films deposited by pulsed laser deposition. *Solid State Sci.* **2008**, *10*, 921–927. [CrossRef]
32. Juma, A.O.; Pistor, P.; Fengler, S.; Dittrich, T.; Wendler, E. Copper diffusion in thin In_2S_3 layers investigated by Rutherford backscattering spectroscopy. *Thin Solid Films* **2012**, *520*, 6740–6743. [CrossRef]
33. Jin, C.; Liu, B.; Lei, Z.; Sun, J. Structure and photoluminescence of the TiO_2 films grown by atomic layer deposition using tetrakis-dimethylamino titanium and ozone. *Nano. Res. Lett.* **2015**, *10*, 1–9.
34. Mercado, C.; Knorr, J.; McHale, L.; Usmani, M.; Ichimura, S.; Saraf, V. Location of Hole and Electron Traps on Nanocrystalline Anatase TiO_2. *J. Phys. Chem. C.* **2012**, *116*, 10796–10804. [CrossRef]
35. Strunk, J.; Vining, C.; Bell, T. A study of oxygen vacancy formation and annihilation in sub monolayer coverages of TiO_2 Dispersed on MCM-48. *J. Phys. Chem. C.* **2010**, *114*, 16937–16945. [CrossRef]